**Mineralogy
and Petrology**

Printed in Austria

# Hydrothermal synthesis of pumpellyite–okhotskite series minerals

**M. Akasaka**[1]**, Y. Suzuki**[1]**, and H. Watanabe**[1,2]

[1] Department of Geoscience, Faculty of Science and Engineering,
Shimane University, Matsue, Japan
[2] Department of Earth Science, Faculty of Science, Kanazawa University,
Kanazawa, Japan

## Summary

Hydrothermal experiments to synthesize pumpellyite group minerals of the pumpellyite–okhotskite series and to investigate their stability have been carried out at 200, 300 and 400 MPa $P_{fluid}$ and 250–500 °C by using cold-seal pressure vessels and solid buffers of $MnO_2$–$Mn_2O_3$, $Cu_2O$–CuO and $Cu_2O$–Cu buffer assemblages. Okhotskite and pumpellyite rich in the okhotskite component crystallized from an oxide mixture starting material of $Ca_4MgMn^{3+}{}_3Al_2Si_6O_{24.5}$-oxide + excess $H_2O$ at $P_{fluid}$ of 200, 300 and 400 MPa and temperatures of 300 and 400 °C. However, a single phase of okhotskite was not produced, and associated piemontite, hausmannite, wollastonite, clinopyroxene, corundum, braunite–neltnerite solid solution and alleghanyite also formed. Mn-pumpellyite of the okhotskite–pumpellyite join occurs as aggregates of needle crystals, rounded grains or flaky crystals. Chemical compositions are variable and range from pumpellyite-($Mn^{2+}$) to okhotskite: 31–36 $SiO_2$, 13–21 $Al_2O_3$, 12–25 total $Mn_2O_3$, 0.6–4 MgO and 20–24 wt.% CaO. Reconnaissance experiments using a starting material of synthetic $Ca_2Mn^{3+}Al_2Si_3O_{12}(OH)$-piemontite at 300 MPa and temperatures of 250, 300, 400 and 500 °C indicate that Mn-rich pumpellyite can crystallize from piemontite at lower temperatures than the stability field of piemontite. The Mn-rich pumpellyite was accompanied by garnet, wollastonite and alleghanyite. The chemical compositions of the Mn-pumpellyites are 32–36 $SiO_2$, 18–27 $Al_2O_3$, 8–18 total $Mn_2O_3$ and 20–23 wt.% CaO. This study shows that the stability fields of piemontite, piemontite + Mn-pumpellyite, and Mn-pumpellyite range in this order with decreasing temperature under high $fO_2$ conditions. The maximum stability temperature of Mn-rich pumpellyite lies between 400 and 500 °C at 200–400 MPa in high $fO_2$ conditions.

## Introduction

Okhotskite $(Ca_8(Mn^{2+}, Mg)_4(Mn^{3+}, Al, Fe^{3+})_8Si_{12}O_{56-n}(OH)_n)$ is an $Mn^{3+}$-dominant pumpellyite group mineral (*Togari* and *Akasaka*, 1987). Okhotskite and Mn-rich pumpellyite of the pumpellyite–okhotskite series have been reported from metamorphosed manganiferous iron ore deposits and Mn-deposits such as the Ochiai mine, Yamanashi prefecture, Japan (*Kato* et al., 1981), the Tokoro belt, Hokkaido, Japan (*Togari* and *Akasaka*, 1987; *Togari* et al., 1988; *Akasaka* et al., 1988), the Sanbagawa belt, Shikoku, Japan (*Minagawa* and *Momoi*, 1990) and the Precambrian Sausar Group, India (*Dasgupta* et al., 1991). Mn-rich pumpellyite has also been found in metamorphosed gabbroic breccia of the Bracco ophiolite, Eastern Liguria, Italy (*Lucchetti*, 1983).

*Akasaka* et al. (1988) and *Togari* et al. (1988) suggested that Mn-pumpellyite is the low temperature equivalent of piemontite, and that Mn-rich pumpellyite group minerals in the manganiferous iron ores from the Tokoro ore deposits formed at about 5 kb and 250–275 °C.

We have been trying to synthesize the Mn-rich pumpellyite group minerals of the pumpellyite–okhotskite series to confirm their crystallization under the metamorphic condition estimated above. Here we describe the preliminary results of our hydrothermal experiments for the synthesis and stability relations of pumpellyite–okhotskite series minerals.


## Experimental methods

For the okhotskite synthesis experiments, we prepared an oxide mixture with a composition of $Ca_4MgMn^{3+}_3Al_2Si_6O_{24.5}$, which satisfies okhotskite stoichiometry. This mixture of $SiO_2$, $Al_2O_3$, $MnO_2$, $MgO$ and $CaCO_3$ was heated in air at 900 °C for one hour to break down carbonate and to convert $Mn^{4+}$ to $Mn^{3+}$. To investigate the stability relationship between piemontite and pumpellyite, $Ca_2Al_2Mn^{3+}Si_3O_{12}(OH)$-piemontite was made by hydrothermal synthesis from an oxide mixture of $Ca_2Al_2Mn^{3+}Si_3O_{12.5}$ + excess $H_2O$ at 200 MPa, 550 °C and $fO_2$ defined by the $MnO_2$–$Mn_2O_3$ solid buffer, for 14 days. Chemical composition of the piemontite was $37.60 \pm 0.30$ $SiO_2$, $19.63 \pm 1.44$ $Al_2O_3$, $17.91 \pm 1.45$ $Mn_2O_3$, $22.49 \pm 0.42$ CaO, with an average total of 97.63 wt.% (n = 7). Its chemical formula is thus $Ca_{1.95}Al_{1.87}Mn^{3+}_{1.10}Si_{3.04}O_{12}(OH)$.

The starting materials were sealed in $Ag_{90}Pd_{10}$ capsules, along with excess distilled $H_2O$. Solid oxygen buffer techniques were employed to produce $fO_2$ adequate to keep manganese in the trivalent state. On the basis of the previous studies of piemontite synthesis by *Anastasiou* and *Langer* (1977) and *Keskinen* and *Liou* (1979), we used $MnO_2$–$Mn_2O_3$, cuprite ($Cu_2O$)–tenorite (CuO) (abbreviated as CT) and cuprite ($Cu_2O$)–copper (Cu) (abbreviated as CC) buffers in our work. Finally, the $Ag_{90}Pd_{10}$ capsules containing the charge were sealed in Ag outer capsules with the buffer mixtures and water.

Hydrothermal experiments were carried out at $P_{fluid}$ of 200, 300 and 400 MPa and temperatures of 250–500 °C, with run durations of 18–35 days, using standard cold-seal pressure vessels produced by High Pressure Chemical Co., Ltd.

The run products were examined using an optical microscope, a JEOL scanning electron microscope equipped with an energy dispersive X-ray spectrometer, a RIGAKU X-ray powder diffractometer (Cu $K_\alpha$ radiation, 35 kV, 25 mA), and a JEOL XMA-8800M electron probe microanalyzer. The electron probe microanalyzer was operated at 15 kV with beam current of $2 \times 10^{-8}$ A and beam diameter of 1 μm. The ZAF method was used for data correction. Standards were natural wollastonite (for Ca and Si), synthetic MnO (Mn), synthetic $Al_2O_3$ (Al) and synthetic MgO (Mg).

## Results of synthesis experiment on $Ca_4MgMn^{3+}{}_3Al_2Si_6O_{24.5}$-oxide mixture + excess $H_2O$

### Phase assemblages

Synthesis data are shown in Table 1. Pumpellyite group minerals of the pumpellyite–okhotskite series (hereafter abbreviated as "Mn-pumpellyite") were produced in all runs. Piemontite, hausmannite, clinopyroxene, wollastonite, corundum, garnet, braunite–neltrerite solid solution (abbreviated as "braunite$_{ss}$") and alleghanyite

Table 1. *Experimental run data for the synthesis of Mn-pumpellyites*

| Run No. | $P_{fluid}$ (MPa) | Temp. (°C) | Buffer | Time (days) | Mineral assemblage[1] |
|---|---|---|---|---|---|
| Starting material: $Ca_4MgMn^{3+}{}_3Al_2Si_6O_{24.5}$-oxide mixture + excess $H_2O$ | | | | | |
| Pum10 | 200 | 400 | $MnO_2$–$Mn_2O_3$ | 31 | Pie + Mn-pum + Hau ( + Cpx + Gt + Wo + Alg) |
| Pum15 | 200 | 400 | $Cu_2O$–Cu | 31 | Pie + Mn-pum + Hau + Cpx ( + Wo + Alg + Gt + Brn) |
| Pum08 | 200 | 300 | $MnO_2$–$Mn_2O_3$ | 31 | Hau + Wo + Mn-pum + Cpx + Alg + Brn |
| Pum06 | 200 | 300 | $Cu_2O$–Cu | 31 | Hau + Mn-pum + Cpx + Wo + Alg ( + Brn) |
| Pum09 | 300 | 400 | $MnO_2$–$Mn_2O_3$ | 30 | Pie + Mn-pum + Cpx + Hau ( + Wo + Alg) |
| Pum14 | 300 | 400 | $Cu_2O$–Cu | 31 | Pie + Cpx + Mn-pum + Hau ( + Gt + Wo + Alg) |
| Pum07 | 300 | 300 | $MnO_2$–$Mn_2O_3$ | 31 | Hau + Mn-pum + Cpx + Pie ( + Wo + Alg + Crd) |
| Pum#2 | 300 | 300 | $Cu_2O$–CuO | 30 | Cpx + Mn-pum + Hau ( + Wo + Alg + Crd) |
| Pum05 | 300 | 300 | $Cu_2O$–Cu | 31 | Mn-pum + Cpx + Hau + Pie ( + Wo + Alg + Crd + Brn) |
| Pum#4 | 400 | 300 | $Cu_2O$–CuO | 30 | Hau + Mn-pum + Cpx ( + Wo + Crd + Alg) |
| Starting material: synthetic $Ca_2Mn^{3+}Al_2Si_3O_{12}(OH)$-piemontite[2] + excess $H_2O$ | | | | | |
| #01 | 300 | 500 | $MnO_2$–$Mn_2O_3$ | 18 | Pie |
| #02 | 300 | 500 | $Cu_2O$–CuO | 18 | Pie |
| Pum13 | 300 | 400 | $MnO_2$–$Mn_2O_3$ | 35 | Mn-Pum + Gt + Wo + Alg[3] |
| Pum16 | 300 | 400 | $Cu_2O$–Cu | 31 | Mn-Pum + Gt + Wo + Alg[3] |
| Pum11 | 300 | 300 | $MnO_2$–$Mn_2O_3$ | 24 | Mn-Pum + Gt + Wo + Alg[3] |
| Pum12 [4] | 300 | 300 | $MnO_2$–$Mn_2O_3$ | 29 | Mn-Pum + Gt + Wo + Alg[3] |
| Pum01 | 300 | 300 | $Cu_2O$–CuO | 27 | Mn-Pum + Brn + Alg ( + An? + Qz)[3] |
| Pum02 | 300 | 250 | $Cu_2O$–Cu | 31 | Mn-Pum + Gt + Wo + Alg[3] |

*Alg* alleghanyite; *An* anorthite; *Brn* braunite; *Cpx* clinopyroxene; *Crd* corundum; *Gt* garnet; *Hau* hausmannite; *Mn-pum* Mn-pumpellyite; *Pie* piemontite; *Qz* quartz; *Wo* wollastonite. [1] Minor phases are shown in parenthesis. [2] Synthesized from $Ca_2Mn^{3+}Al_2Si_3O_{12.5}$-oxide mixture + $H_2O$ at 200 MPa and 550 °C using $MnO_2$–$Mn_2O_3$ buffer. [3] Piemontite starting material still present. [4] Starting material: Product of No. Pum11

Fig. 1. Starting materials, synthetic phases and end members of solid solutions in the system $CaO-MgO-MnO-Mn_2O_3-Al_2O_3-SiO_2-H_2O$ plotted from $SiO_2$, $H_2O$ and $O_2$ in the Ca–Mg–Mn–Al tetrahedron

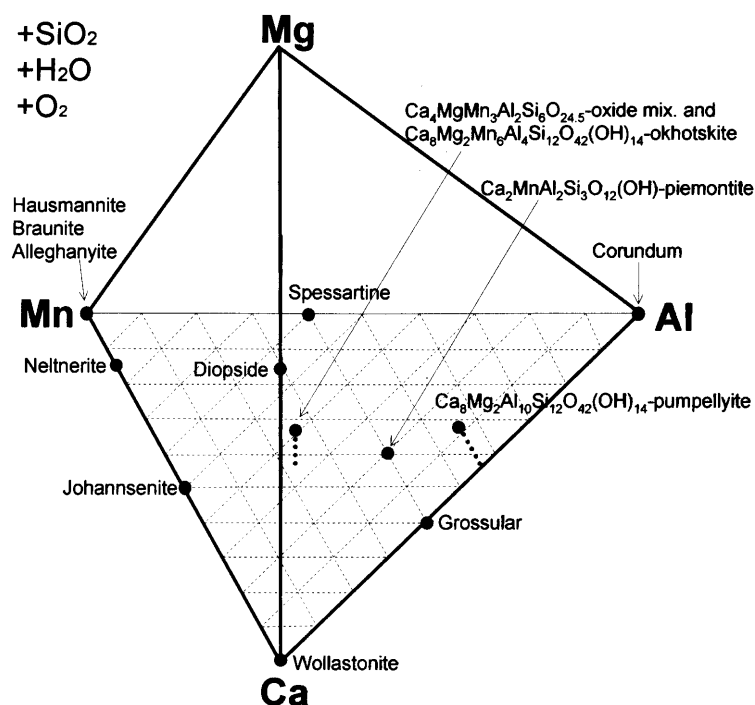were associated phases. In Fig. 1, starting materials, synthetic phases and end members of solid solutions in the system $CaO-MgO-MnO-Mn_2O_3-Al_2O_3-SiO_2-H_2O$ are plotted from $SiO_2$, $H_2O$ and $O_2$ in the Ca–Mg–Mn–Al tetrahedron.

At 200 MPa $P_{fluid}$ and 400 °C, the assemblage piemontite + Mn-pumpellyite + hausmannite + clinopyroxene was produced, along with minor phases such as wollastonite, alleghanyite, garnet, ± braunite$_{ss}$. At 200 MPa $P_{fluid}$ and 300 °C, the phase assemblage was hausmannite + wollastonite + Mn-pumpellyite + clinopyroxene + alleghanyite + braunite$_{ss}$. Piemontite appeared at 400 °C, but was absent at 300 °C.

Hausmannite formed even in the run products buffered by the $MnO_2-Mn_2O_3$ solid buffer assemblage, indicating that $fO_2$ was lower than that defined by that solid buffer. *Keskinen* and *Liou* (1979) examined the effect of solid buffers at low temperatures, and concluded that at temperatures less than 400 °C, solid buffers are ineffective in controlling $fO_2$, at least in the early stages of runs, because of the very low diffusion rate of $H_2$ at low temperatures. Moreover, in his study of synthesis of piemontite *Strens* (1966) pointed out that when oxide mixtures containing Mn-oxide are used as starting material, Mn-oxide recrystallizes rapidly, with consequent immobilization of the manganese and formation of epidote or clinozoisite. Thus, we consider that the solid buffers were not effective in the early stages of the run, and reduced conditions were produced in the
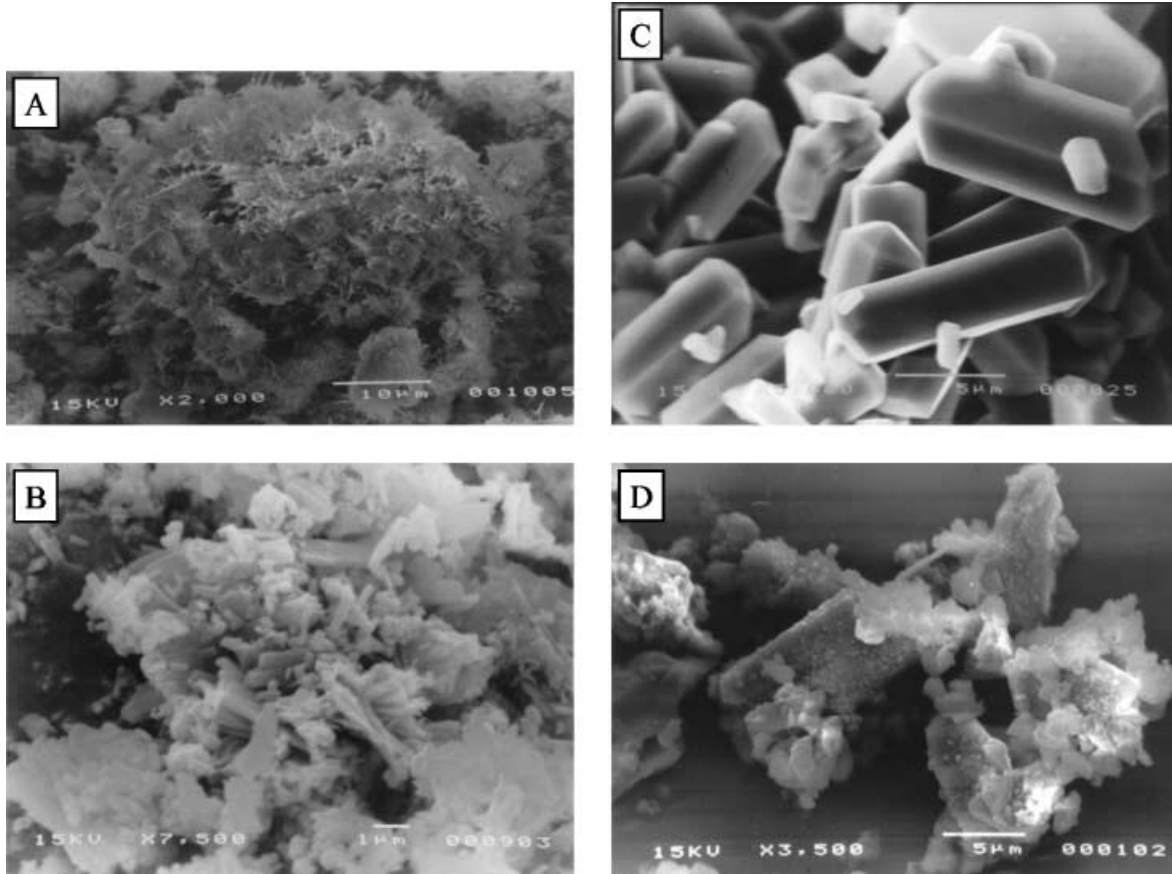
Fig. 2. SEM images of run products. **A** Aggregates of needle crystals of Mn-pumpellyite crystallized at 200 MPa $P_{fluid}$ and temperatures of 400 °C (Run No. Pum10). Scale bar is 10 μm. **B** Prismatic crystals of piemontite crystallized at 300 MPa $P_{fluid}$ and temperatures of 400 °C (Run No. Pum09). Scale bar is 1 μm. **C** Prismatic crystals of $Ca_2Mn^{3+}$ $Al_2Si_3O_{12}(OH)$-piemontite starting material. Scale bar is 5 μm. **D** Run product from $Ca_2Mn^{3+}Al_2Si_3O_{12}(OH)$-piemontite + excess $H_2O$ at 300 MPa $P_{fluid}$ and temperatures of 300 °C (Run No. Pum12). Scale bar is 5 μm

inner capsule by the elevated pressure and temperature, causing rapid crystallization of hausmannite. However, the formation of hausmannite indicates that $fO_2$ conditions in which both of $Mn^{2+}$ and $Mn^{3+}$ were present prevailed during the run.

In run products at 300 MPa $P_{fluid}$, temperatures of 400 and 300 °C, and using $MnO_2$–$Mn_2O_3$ and CC buffers, both piemontite and Mn-pumpellyite were formed, along with associated minerals. The amount of piemontite at 300 °C is considerably less than that at 400 °C, whereas the amount of Mn-pumpellyite at 300 °C is greater than that at 400 °C. In the 300 °C CT-buffered run product, Mn-pumpellyite was formed along with other phases, but no piemontite formed.

Crystallization of Mn-pumpellyite was also confirmed in the run product at 400 MPa $P_{fluid}$ and 300 °C using CT buffer.

Table 2. *Average chemical compositions of Mn-pumpellyites and piemontites crystallized from $Ca_4MgMn^{3+}_3Al_2Si_6O_{24.5}$-oxide mixture + excess $H_2O$*

| | Mn-pumpellyite | | | | | | | | | | | | Piemontite | | | |
|---|---|---|---|---|---|---|---|---|---|---|---|---|---|---|---|---|
| $P_{fluid}$ | 300 MPa | | | | | | 200 MPa | | | | | | 300 MPa | | 200 MPa | |
| Temp. | 300 °C | | | | | | 400 °C | | | | | | 400 °C | | 400 °C | |
| Buffer Run No. | Cu₂O–CuO Pum#2 | | MnO₂–Mn₂O₃ Pum07 | | Cu₂O–Cu Pum14 | | MnO₂–Mn₂O₃ Pum09 | | Cu₂O–Cu Pum15 | | MnO₂–Mn₂O₃ Pum10 | | MnO₂–Mn₂O₃ Pum09 | | MnO₂–Mn₂O₃ Pum10 | |
| | Av. n=4 | s.d. | Av. n=6 | s.d. | Av. n=5 | s.d. | Av. n=4 | s.d. | Av. n=5 | s.d. | Av. n=3 | s.d. | Av. n=8 | s.d. | Av. n=4 | s.d. |
| $SiO_2$ | 34.15 | 2.18 | 35.19 | 1.26 | 35.24 | 1.34 | 34.56 | 1.71 | 35.19 | 1.04 | 36.24 | 0.28 | 37.25 | 0.64 | 37.06 | 1.04 |
| $Al_2O_3$ | 11.11 | 1.94 | 15.61 | 1.04 | 14.27 | 1.28 | 15.23 | 1.96 | 16.47 | 2.08 | 14.58 | 1.87 | 19.10 | 0.56 | 18.27 | 1.51 |
| $Mn_2O_3$ * | 21.92 | 5.35 | 18.32 | 3.31 | 17.92 | 1.78 | 18.58 | 5.25 | 15.80 | 2.54 | 14.83 | 0.57 | 15.53 | 0.66 | 17.44 | 2.31 |
| $MgO$ | 3.21 | 0.36 | 1.78 | 0.15 | 2.26 | 0.65 | 1.30 | 0.60 | 1.92 | 0.80 | 2.85 | 0.83 | 0.39 | 0.04 | 0.69 | 0.07 |
| $CaO$ | 21.03 | 0.83 | 22.09 | 1.07 | 22.16 | 0.60 | 21.14 | 0.42 | 21.91 | 0.90 | 22.26 | 0.28 | 23.72 | 0.75 | 24.25 | 0.39 |
| Total | 91.42 | | 92.99 | | 91.85 | | 90.81 | | 91.29 | | 90.76 | | 95.99 | | 97.71 | |
| **Cations per total cations = 32** | | | | | | | | | | | | | **Cations per 12.5 oxygens** | | | |
| Si | 11.98 | 0.79 | 12.00 | 0.32 | 12.14 | 0.28 | 12.12 | 0.57 | 12.11 | 0.27 | 12.50 | 0.07 | 3.06 | 0.01 | 3.02 | 0.05 |
| Al | 4.60 | 0.86 | 6.27 | 0.43 | 5.80 | 0.43 | 6.30 | 0.83 | 6.67 | 0.82 | 5.92 | 0.80 | 1.85 | 0.03 | 1.75 | 0.13 |
| Mn | 5.84 | 1.38 | 4.76 | 0.88 | 4.71 | 0.52 | 4.96 | 1.40 | 4.15 | 0.81 | 3.90 | 0.15 | 0.97 | 0.05 | 1.08 | 0.15 |
| Mg | 1.68 | 0.18 | 0.90 | 0.08 | 1.17 | 0.34 | 0.68 | 0.31 | 0.99 | 0.49 | 1.46 | 0.49 | 0.05 | 0.00 | 0.08 | 0.01 |
| Ca | 7.90 | 0.34 | 8.07 | 0.21 | 8.18 | 0.14 | 7.94 | 0.15 | 8.08 | 0.22 | 8.22 | 0.13 | 2.09 | 0.07 | 2.12 | 0.04 |
| **Structural formula (total cations = 32)** | | | | | | | | | | | | | | | | |
| Si | 11.98 | | 12.00 | | 12.14 | | 12.12 | | 12.11 | | 12.50 | | | | | |
| Al | 0.02 | | 0.00 | | 0.00 | | 0.00 | | 0.00 | | 0.00 | | | | | |
| Z | 12.00 | | 12.00 | | 12.14 | | 12.12 | | 12.11 | | 12.50 | | | | | |
| Al | 4.58 | | 6.27 | | 5.80 | | 6.30 | | 6.67 | | 5.92 | | | | | |
| $Mn^{3+}$ | 3.42 | | 1.73 | | 2.20 | | 1.70 | | 1.33 | | 2.08 | | | | | |
| Y | 8.00 | | 8.00 | | 8.00 | | 8.00 | | 8.00 | | 8.00 | | 8.02 | | 8.05 | |
| $Mn^{2+}$ | 2.32 | | 3.03 | | 2.51 | | 3.26 | | 2.82 | | 1.82 | | | | | |
| Mg | 1.68 | | 0.90 | | 1.17 | | 0.68 | | 0.99 | | 1.46 | | | | | |
| X | 4.00 | | 3.93 | | 3.68 | | 3.94 | | 3.81 | | 3.28 | | | | | |
| Mn | 0.10 | | 0.00 | | 0.00 | | 0.00 | | 0.00 | | 0.00 | | | | | |
| Ca | 7.90 | | 8.07 | | 8.18 | | 7.94 | | 8.08 | | 8.22 | | | | | |
| W | 8.00 | | 8.07 | | 8.18 | | 7.94 | | 8.08 | | 8.22 | | | | | |

* Total Mn as $Mn_2O_3$

*Crystalline phases*

1) *Mn-pumpellyite of the pumpellyite–okhotskite series.* Mn-pumpellyite occurs as aggregates of needle crystals (Fig. 2A), rounded grains or flaky crystals. The Mn-pumpellyite grains are brownish under the optical microscope.

   X-ray powder diffraction analysis identified the Mn-pumpellyite as okhotskite by reflections with $d$-spacings (Å) of 4.76 (004, 111), 4.43 ($\bar{1}$04, 200), 3.87 (202), 3.43 (211), 3.09 (204), 3.03 (020), 2.96 (115, 300), 2.88 (022), 2.72 (302), 2.67 ($\bar{3}$04, $\bar{3}$11), 2.55 (024, $\bar{3}$13) and others.

   Average compositions of the synthesized Mn-pumpellyites are listed in Table 2, with structural formulae, $W_8X_4Y_8Z_{12}O_{56-n}(OH)_n$, calculated on the basis of 32 cations, where $W$, $X$, $Y$ and $Z$ are 7-, 6-, 6- and 4-coordinated sites, respectively. Mn in the $X$-site is represented as $Mn^{2+}$, after the method by *Kato* et al. (1981) and *Togari* and *Akasaka* (1987), although some Mn in the $X$-site may be trivalent (*Akasaka* et al., 1997). Mn in the $Y$-site is $Mn^{3+}$ (*Kato* et al., 1981; *Togari* and *Akasaka*, 1987; *Artioli* et al., 1996; *Akasaka* et al., 1997). The compositional ranges between Al and $Mn^{3+}$ in the $Y$-site and between Mg and $Mn^{2+}$ in the $X$-site are shown in Fig. 3. Although Al and $Mn^{3+}$ in the $Y$-site are variable, $Mn^{3+}$ reaches more than 50% $Y$-site occupancy in the Mn-pumpellyite produced at 300 MPa and 300 °C. Thus, these Mn-pumpellyites are okhotskite. Even in the Mn-pumpellyites where $Mn^{3+}$ occupies less than half of the $Y$-site, maximum $Mn^{3+}{}_Y$-contents are close to those of okhotskite.

   Mg and Mn in the $X$-site are also variable; Mg ranges between 0.2 to 2.0 atoms per formula unit (apfu), and Mn between 1.2 to 3.6 apfu. However, the Mg:Mn-ratio in the $X$-site of okhotskite synthesized at 300 MPa and 300 °C using the CT buffer is close to that of the starting material.

2) *Other phases.* Piemontite produced at 400 °C was prismatic, as shown by the SEM image (Fig. 2B). Average chemical compositions at 400 °C are shown
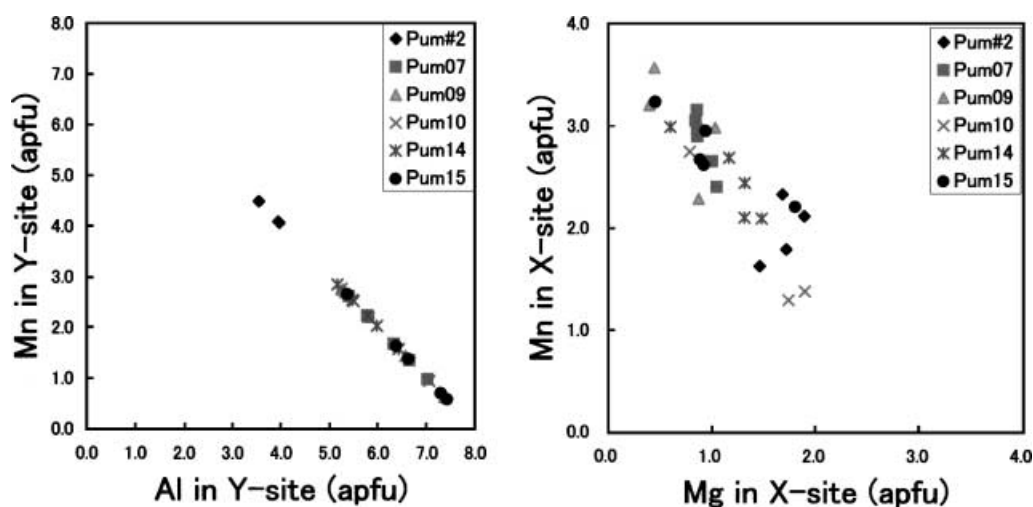


Fig. 3. Al–Mn in *Y*-site and Mg–Mn in *X*-site diagrams of Mn-pumpellyites in run products

Table 3. *Average chemical compositions of Mn-pumpellyites crystallized from $Ca_2Mn^{3+}Al_2Si_3O_{12}(OH)$-piemontite $+ H_2O$ at 300 MPa $P_{fluid}$*

| $P_{fluid}$ | 300 MPa | | | | | | | | | |
|---|---|---|---|---|---|---|---|---|---|---|
| Temp. | 250 °C | | 300 °C | | | | 400 °C | | | |
| Buffer | $Cu_2O$–Cu | | $Cu_2O$–CuO | | $MnO_2$–$Mn_2O_3$ | | $Cu_2O$–Cu | | $MnO_2$–$Mn_2O_3$ | |
| Run No. | Pum02 | | Pum01 | | Pum12 | | Pum16 | | Pum13 | |
| | Av. n = 10 | s.d. | Av. n = 5 | s.d. | Av. n = 4 | s.d. | Av. n = 6 | s.d. | Av. n = 6 | s.d. |
| $SiO_2$ | 34.63 | 0.74 | 34.17 | 0.58 | 33.76 | 0.36 | 34.72 | 1.07 | 33.88 | 1.46 |
| $Al_2O_3$ | 19.72 | 0.43 | 20.23 | 0.48 | 19.30 | 0.47 | 22.19 | 1.19 | 20.91 | 2.56 |
| $Mn_2O_3$* | 16.15 | 0.61 | 17.40 | 0.46 | 15.71 | 1.39 | 12.63 | 1.48 | 14.29 | 3.85 |
| CaO | 22.33 | 0.35 | 21.36 | 0.95 | 21.51 | 0.89 | 22.24 | 1.05 | 21.85 | 0.99 |
| Total | 92.83 | | 93.16 | | 90.28 | | 91.78 | | 90.93 | |
| Cations per total cations = 32 | | | | | | | | | | |
| Si | 11.78 | 0.16 | 11.65 | 0.22 | 11.80 | 0.04 | 11.78 | 0.28 | 11.67 | 0.20 |
| Al | 7.90 | 0.14 | 8.66 | 0.66 | 7.96 | 0.16 | 8.87 | 0.40 | 8.49 | 0.83 |
| Mn | 4.18 | 0.15 | 3.84 | 1.10 | 4.18 | 0.40 | 3.27 | 0.41 | 3.77 | 1.08 |
| Ca | 8.14 | 0.11 | 7.85 | 0.26 | 8.06 | 0.27 | 8.08 | 0.32 | 8.07 | 0.14 |
| Structural formula (total cations = 32) | | | | | | | | | | |
| Si | 11.78 | | 11.65 | | 11.80 | | 11.78 | | 11.67 | |
| Al | 0.22 | | 0.35 | | 0.20 | | 0.22 | | 0.33 | |
| Z | 12.00 | | 12.00 | | 12.00 | | 12.00 | | 12.00 | |
| Al | 7.68 | | 8.00 | | 7.76 | | 8.00 | | 8.00 | |
| $Mn^{3+}$ | 0.32 | | 0.00 | | 0.24 | | 0.00 | | 0.00 | |
| Y | 8.00 | | 8.00 | | 8.00 | | 8.00 | | 8.00 | |
| Al | 0.00 | | 0.31 | | 0.00 | | 0.65 | | 0.16 | |
| $Mn^{2+}$ | 3.86 | | 3.69 | | 3.94 | | 3.27 | | 3.77 | |
| X | 3.86 | | 4.00 | | 3.94 | | 3.92 | | 3.93 | |
| Mn | 0.00 | | 0.15 | | 0.00 | | 0.00 | | 0.00 | |
| Ca | 8.14 | | 7.85 | | 8.06 | | 8.08 | | 8.07 | |
| W | 8.14 | | 8.00 | | 8.06 | | 8.08 | | 8.07 | |

* Total Mn as $Mn_2O_3$

in Table 2. They lie in the range $Ca_2Al_2Mn^{3+}Si_3O_{12}(OH)$–$Ca_2Al_{1.5}Mn^{3+}_{1.5}$ $Si_3O_{12}(OH)$; this compositional range is very similar to that of natural piemontite coexisting with Mn-pumpellyite (*Akasaka* et al., 1988). Clinopyroxenes are a solid solution of the diopside–johannsenite join; they also contain small amounts of $CaMn^{3+}AlSiO_6$ and $CaAlAlSiO_6$ components. The garnet is grossular, which contains up to about 17% $Mn^{3+}$ in the octahedral site, and has a spessartine component of up to about 30 mol.%. Braunite$_{ss}$ is a solid solution of $CaMn^{3+}_6SiO_{12}$, $Mn^{2+}Mn^{3+}_6SiO_{12}$ and $MgMn^{3+}_6SiO_{12}$ components.
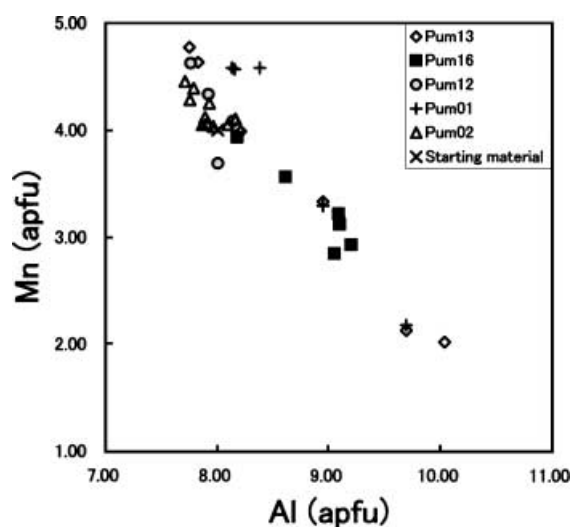
## Results of stability experiments on $Ca_2Mn^{3+}Al_2Si_3O_{12}(OH)$-piemontite + excess $H_2O$

*Phase assemblages*

Figure 2C shows the SEM images of piemontite crystals of the starting material. At 300 MPa $P_{fluid}$ and 500 °C, the starting material was unchanged; thus, piemontite is stable under these conditions. However, at temperatures of 400, 300 and 250 °C, the assemblage Mn-pumpellyite + wollastonite + garnet + alleghanyite grew at the expense of piemontite. The Mn-pumpellyite was identified as pumpellyite-($Mn^{2+}$) or okhotskite by X-ray powder diffraction. Figure 2D shows the dissolved nature of piemontite after the run using $MnO_2$–$Mn_2O_3$ buffer at 300 MPa $P_{fluid}$ and 300 °C. Nevertheless, considerable amounts of piemontite remained after reaction. The run product heated at 300 °C for 24 days using $MnO_2$–$Mn_2O_3$ buffer (Run No. Pum11) was reheated at the same pressure and temperature for another 29 days (Run No. Pum12). The amounts of Mn-pumpellyite and garnet relative to piemontite increased with longer duration, but the mineral assemblage did not change.

*Crystalline phases*

1) *Mn-pumpellyite*. Average compositions of this phase are shown in Table 3. Mn in the *X*- and *Y*-sites is represented as $Mn^{2+}$ and $Mn^{3+}$, respectively, as explained above. Since $Al^{3+}$ is the dominant cation in the *Y*-site, the present phase should be called pumpellyite-($Mn^{2+}$). The variations of Al and Mn (apfu) of Mn-pumpellyites in each run are plotted in Fig. 4. The Al- and Mn-ranges of Mn-pumpellyites from Runs Pum13 and Pum16 at 400 °C and from Run Pum01 at 300 °C are considerably wider than those from Run Pum12 at 300 °C and Pum02 at 250 °C, and extend to the Al-rich side to as much as about



Fig. 4. Al–Mn variation in Mn-pumpellyites crystallized from synthetic $Ca_2Mn^{3+}Al_2\,Si_3\,O_{12}\,(OH)$ - piemontite + $H_2O$

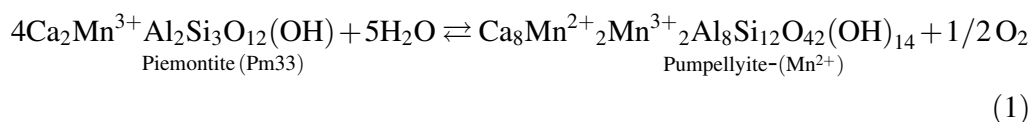10 apfu Al. This corresponds to the increase of Al in the $X$-site, as shown by the structural formula in Table 3.

2) *Other phases*. Garnet of the grossular (Gr)–spessartine (Sp) solid solution occurred as dodecahedral crystals. The chemical compositions of garnets crystallized at 250, 300 and 400 °C are $Gr_{66}Sp_{34}$–$Gr_{92}Sp_8$, $Gr_{64}Sp_{36}$–$Gr_{65}Sp_{35}$ and $Gr_{55}Sp_{45}$–$Gr_{66}Sp_{34}$ (mol%), respectively. Although wollastonite and alleghanyite were identified in all run products by X-ray powder diffraction, EPMA analyses were unsuccessful.
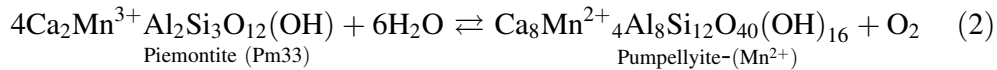
## Discussion

*Interpretation of the experimental results*

The attainment of equilibrium in the hydrothermal experiments at temperatures below 400 °C would be hampered by the low crystallization rate and the very low diffusion rate of $H_2$. Moreover, the crystallization of synthetic pumpellyite is strongly dependent on fluid pressure: $Ca_4MgAl_5Si_6O_{21}(OH)_7$-pumpellyite has been synthesized at 600–900 MPa and 275–410 °C (*Hinrichsen* and *Schümann*, 1969; *Schiffman* and *Liou*, 1980) and Fe-pumpellyite at 500–910 MPa and 275–325 °C (*Schiffman* and *Liou*, 1983), but not at lesser pressures. The nature of the starting material also has an effect on the synthetic phases or assemblages crystallized in the synthesis experiments. *Schiffman* and *Liou* (1980) showed that pumpellyite-bearing assemblages were formed from charges with crystalline mixtures, but not from those with amorphous gel, and *Strens* (1966) mentioned that Mn-oxide would recrystallize rapidly from oxide mixtures in the early stages of runs. Thus, as *Schiffman* and *Liou* (1980) pointed out, discerning the significant contributions of various non-equilibrium constraints on crystallization would require very carefully conceived and executed experimentation. In spite of these difficulties for the synthesis experiments, pumpellyite–okhotskite series minerals were synthesized from the oxide mixture at pressures of 200–400 MPa and temperatures of 250–400 °C in the present study, although okhotskite was not obtained as a single phase.

The present reconnaissance experiments using a starting material of synthetic $Ca_2Mn^{3+}Al_2Si_3O_{12}(OH)$-piemontite indicate that Mn-rich pumpellyite can crystallize from piemontite at temperatures lower than the stability field of piemontite, and suggest that the maximum stability temperature of Mn-rich pumpellyite would lie between 400 and 500 °C at high $fO_2$ condition. It has been known that the high temperature equivalent of Mg–Al–pumpellyite is zoisite + grossular + amesite + quartz + $H_2O$ (*Hinrichsen* and *Schürmann*, 1969) or clinozoisite + grossular + chlorite + quartz + $H_2O$ (*Schiffman* and *Liou*, 1980), and that of Fe-pumpellyite is epidote ± minor amounts of chlorite, garnet, quartz, hematite and magnetite (*Schiffman* and *Liou*, 1983). Thus, the present result is consistent with the general phase relations between epidote-group minerals and pumpellyite-group minerals. The crystallization of pumpellyite-($Mn^{2+}$) from piemontite is represented by:

$$4Ca_2Mn^{3+}Al_2Si_3O_{12}(OH) + 5H_2O \rightleftarrows Ca_8Mn^{2+}{}_2Mn^{3+}{}_2Al_8Si_{12}O_{42}(OH)_{14} + 1/2\,O_2$$

Piemontite (Pm33)  Pumpellyite-($Mn^{2+}$)

(1)

as proposed by *Akasaka* et al. (1988), or

$$4Ca_2Mn^{3+}Al_2Si_3O_{12}(OH) + 6H_2O \rightleftharpoons Ca_8Mn^{2+}{}_4Al_8Si_{12}O_{40}(OH)_{16} + O_2 \quad (2)$$

Piemontite (Pm33)        Pumpellyite-(Mn$^{2+}$)

However, the assemblage of run products in the present experiments is not explained by such simple reactions. Further experiments are necessary to identify the low temperature equivalent of piemontite at low temperatures.

*Application to natural pumpellyite–okhotskite series minerals*

Mineral assemblages including piemontite and Mn-pumpellyite have been reported from several localities. Piemontite and Mn-rich pumpellyite coexist in quartz veinlets in the Tokoro manganiferous iron ores, whereas okhotskite-veinlets crosscut veinlets of piemontite or piemontite + Mn-rich pumpellyite (*Togari* and *Akasaka*, 1987; *Togari* et al., 1988; *Akasaka* et al., 1988). On the basis of the present study, we interpret these occurrences as follows: piemontite crystallized at temperatures above the upper limit of Mn-pumpellyite stability, followed by the formation of the assemblage piemontite + Mn-rich pumpellyite with decreasing temperature, and okhotskite formed at temperatures below the lower limit of piemontite stability. *Akasaka* et al. (1988) and *Togari* et al. (1988) suggested that the above minerals formed at about 500 MPa $P_{fluid}$ and 250–275 °C which are metamorphic conditions estimated for the metabasite, the footwall of the Tokoro ore deposits, by *Sakakibara* (1986). Our experimental results showing that piemontite, pumpellyite-(Mn$^{2+}$) and okhotskite crystallize at 200–400 MPa $P_{fluid}$ and 250–400 °C under high $fO_2$ conditions are reasonably consistent with the estimated metamorphic conditions.

In the Ochiai mine, piemontite and pumpellyite-(Mn$^{2+}$) occur in a massive braunite ore. *Kato* et al. (1981) considered that the ores had suffered laumontite + prehnite–pumpellyite facies metamorphism, based on the metamorphic conditions of the pyroclastic rocks around the ore deposit. Furthermore, *Minagawa* and *Momoi* (1990) reported mineral assemblages consisting of braunite, hematite, piemontite, okhotskite and associated minerals from Sanbagawa manganese ore deposits which suffered glaucophane–greenschist facies metamorphism. The crystallization conditions of piemontite and Mn-pumpellyite in these ore deposits seem to be similar to those in the Tokoro manganiferous iron ore deposits.

Mn-rich minerals of the pumpellyite group occur in Mn oxide ores of the Precambrian Sausar Group, India (*Dasgupta*, 1991). Although piemontite occurs at the contact of pegmatite dikes and the ores, it is not present in the mineral assemblages containing pumpellyite: braunite + K-feldspar + pumpellyite + calcite ± bixbyite and braunite + phlogopite + pumpellyite + calcite ± diopside ± bixbyite. The lack of piemontite suggests that these assemblages formed at temperatures less than 300 °C.

It is also notable that the reduced assemblages in the present experiments made up of Mn$^{2+}$-bearing minerals, such as clinopyroxene and alleghanyite, are similar to those in nature. In the Tokoro ore deposits, johannsenite, bementite ($Mn_8Si_6O_{15}(OH)_{10}$) and inesite ($Ca_2Mn_7Si_{10}O_{28}(OH)_2 \cdot 5H_2O$) formed in the later stages, indicating decrease of $fO_2$ (*Togari* et al., 1988). *Kato* et al. (1981) also described ore from the Ochiai mine which consisted mainly of massive caryopilite

$((Mn, Mg)_3Si_2O_5(OH)_4)$ with minor quartz, johannsenite and rhodochrosite. Bementite and caryopilite can be attributed to alleghanyite in the present run products. Thus, even if metamorphic pressure and temperature were constant, different mineral assemblages would be obtained by change of $fO_2$ or by local $fO_2$ conditions.

## Conclusions

(1) Mn-rich pumpellyite group minerals of the pumpellyite–okhotskite series were synthesized from $Ca_4MgMn^{3+}_3Al_2Si_6O_{24.5}$ oxide mixture + excess $H_2O$ at 200–400 MPa $P_{fluid}$ and temperatures of 300–400 °C, using solid buffers such as $MnO_2$–$Mn_2O_3$, $Cu_2O$–CuO and $Cu_2O$–Cu buffer assemblages. However, they did not crystallize as a single phase because of significant non-equilibrium constraints on crystallization.

(2) Reconnaissance experiments using a starting material of synthetic $Ca_2Mn^{3+}$ $Al_2Si_3O_{12}(OH)$-piemontite indicate that Mn-rich pumpellyite can crystallize from piemontite at lower temperatures than the stability field of piemontite, and suggest that the maximum stability temperature of Mn-rich pumpellyite lies between 400 and 500 °C at 300 MPa in high $fO_2$ conditions.

(3) The stability fields of piemontite, piemontite + Mn-pumpellyite and Mn-pumpellyite range in this order with decreasing temperature under high $fO_2$ conditions. This relationship is consistent with the general phase relations between epidote-group minerals and pumpellyite-group minerals.

## References

*Akasaka M, Sakakibara M, Togari K* (1988) Piemontite from the manganiferous hematite ore deposits in the Tokoro Belt, Hokkaido, Japan. Mineral Petrol 38: 105–116

*Akasaka M, Kimura Y, Omori Y, Sakakibara M, Shinno I, Togari K* (1997) [57]Fe Mössbauer study of pumpellyite–okhotskite–julgoldite series minerals. Mineral Petrol 61: 181–198

*Anastasiou P, Langer K* (1977) Synthesis and physical properties of piemontite $Ca_2Al_{3-p}$ $Mn^{3+}_p(Si_2O_7/SiO_4/O/OH)$. Contrib Mineral Petrol 60: 225–245

*Artioli G, Pavese A, Bellotto M, Collins SP, Lucchetti G* (1996) Mn crystal chemistry in pumpellyite: a resonant-scattering powder diffraction Rietveld study using synchrotron radiation. Am Mineral 81: 603–610

*Dasgupta S, Chakraborti S, Sengupta P, Bhattacharya PK, Banerjee H, Roy S, Fukuoka M* (1991) Manganese-rich minerals of the pumpellyite group from the Precambrian Sausar Group, India. Am Mineral 76: 241–245

*Hinrichsen T, Schürmann K* (1969) Untersuchungen zur Stabilität von Pumpellyit. N Jb Mineral Mh 10: 131–132

*Kato A, Matsubara S, Yamamoto R* (1981) Pumpellyite-($Mn^{2+}$) from the Ochiai Mine, Yamanashi Prefecture, Japan. Bull Minèral 104: 396–399

*Keskinen M, Liou JG* (1979) Synthesis and stability relations of Mn–Al piemontite, $Ca_2Mn$ $Al_2Si_3O_{12}(OH)$. Am Mineral 64: 317–328

*Liou JG* (1979) Zeolite facies metamorphism of basaltic rocks from the east Taiwan ophiolite. Am Mineral 64: 1–14

*Lucchetti G* (1983) Mn-rich pumpellyite from Eastern Liguria (Italy). N Jb Mineral Mh 12: 563–568

*Minagawa T, Momoi H* (1990) Okhotskite from bedded manganese ore deposits from the Sanbagawa metamorphic belt, Shikoku. Annual Meeting of Mineral Soc Japan, pp 87 (in Japanese)

*Passaglia E, Gottardi G* (1973) Crystal chemistry and nomenclature of pumpellyites and julgoldites. Can Mineral 12: 219–223

*Sakakibara M* (1986) A newly discovered high-pressure terrane in eastern Hokkaido, Japan. J Metamorph Geol 4: 401–408

*Schiffman P, Liou JG* (1980) Synthesis and stability relations of Mg–Al pumpellyite $Ca_4Al_5MgSi_6O_{21}(OH)_7$. J Petrol 21: 441–474

*Schiffman P, Liou JG* (1983) Synthesis of Fe-pumpellyite and its stability relations with epidote. J Metamorph Geol 1: 91–101

*Strens RGJ* (1966) Synthesis and properties of piemontite. Nature 201: 175–176

*Togari K, Akasaka M* (1987) Okhotskite, a new mineral, an $Mn^{3+}$-dominant member of the pumpellyite group, from the Kokuriki mine, Hokkaido, Japan. Mineral Mag 51: 611–614

*Togari K, Akasaka M, Sakakibara M, Watanabe T* (1988) Mineralogy of manganiferous iron ore deposits and chert from the Tokoro Belt, Hokkaido. Mining Geol Spec Issue 12: 115–126

Authors' addresses: Dr. *M. Akasaka* and *Y. Suzuki*, Department of Geoscience, Interdisciplinary Faculty of Science and Engineering, Shimane University, 1060 Nishikawatsu, Matsue 690-8504, Japan, e-mail: akasaka@riko.shimane-u.ac.jp; *H. Watanabe*, Department of Earth Science, Faculty of Science, Kanazawa University, Kanazawa, 920-1192, Japan